Figure 1: Three Theoretical Frameworks as Perspectives on Universal Optimization Principle

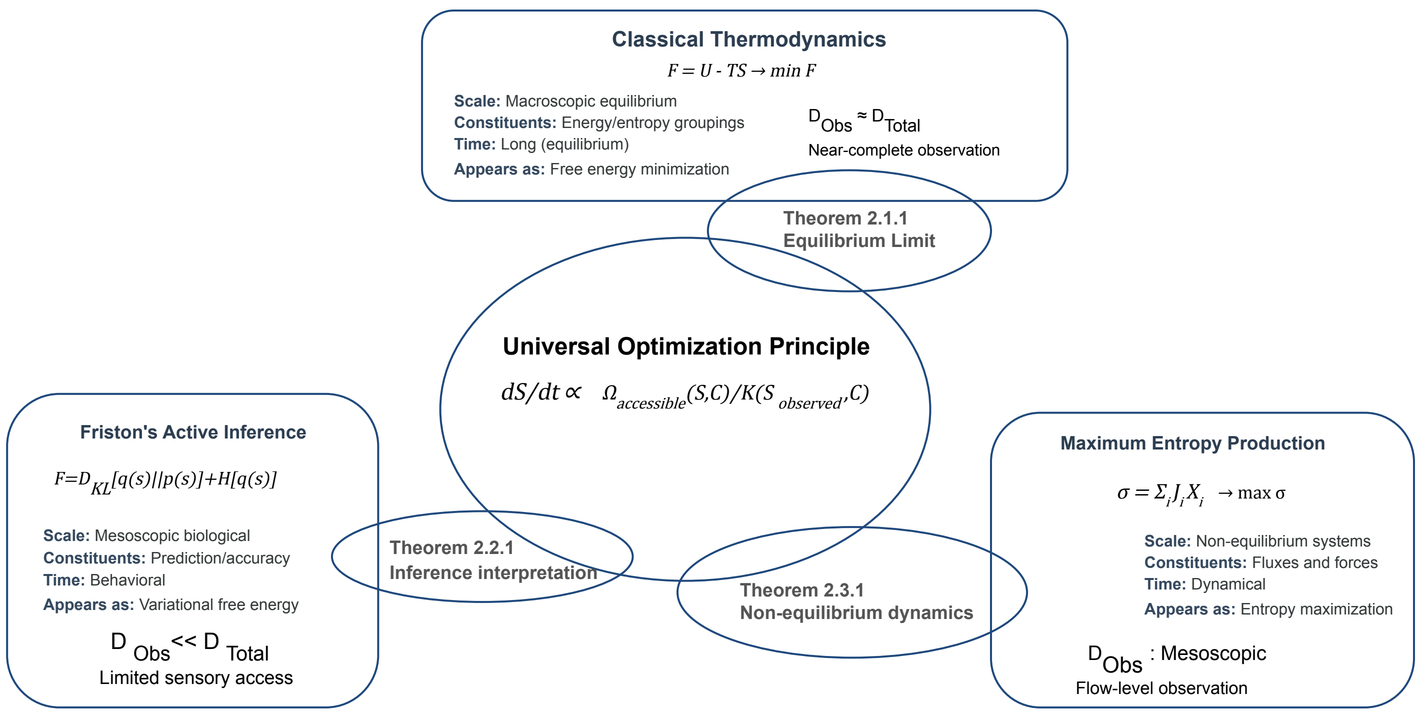

Figure 1. Universal optimization principle underlying three major theoretical frameworks. **Central panel:** The universal optimization of $\Omega_{accessible}/K(S_{observed})$, where systems maximize entropy production through accessible configuration exploration while minimizing trajectory complexity. The network visualization represents the multi-pathway nature of system evolution. **Surrounding panels:** Three different observational perspectives on the same underlying process: Classical thermodynamics observes near-equilibrium with complete state access ($D_{obs} \approx D_{total}$), Friston's framework observes through sensory boundaries with limited access ($D_{obs} << D_{total}$), and MEPP observes dissipative dynamics at mesoscopic scales. **Arrows:** Mathematical equivalence relationships (Theorems 2.1.1,2.2.1,,2.3.1) demonstrate these are not different phenomena but different constituent construction frameworks C for observing the same universal optimization. The apparent differences arise from varying D_{obs}/D_{total} ratios and measurement timescales. The pulsing animation of the central core represents the dynamic nature of entropy production optimization.

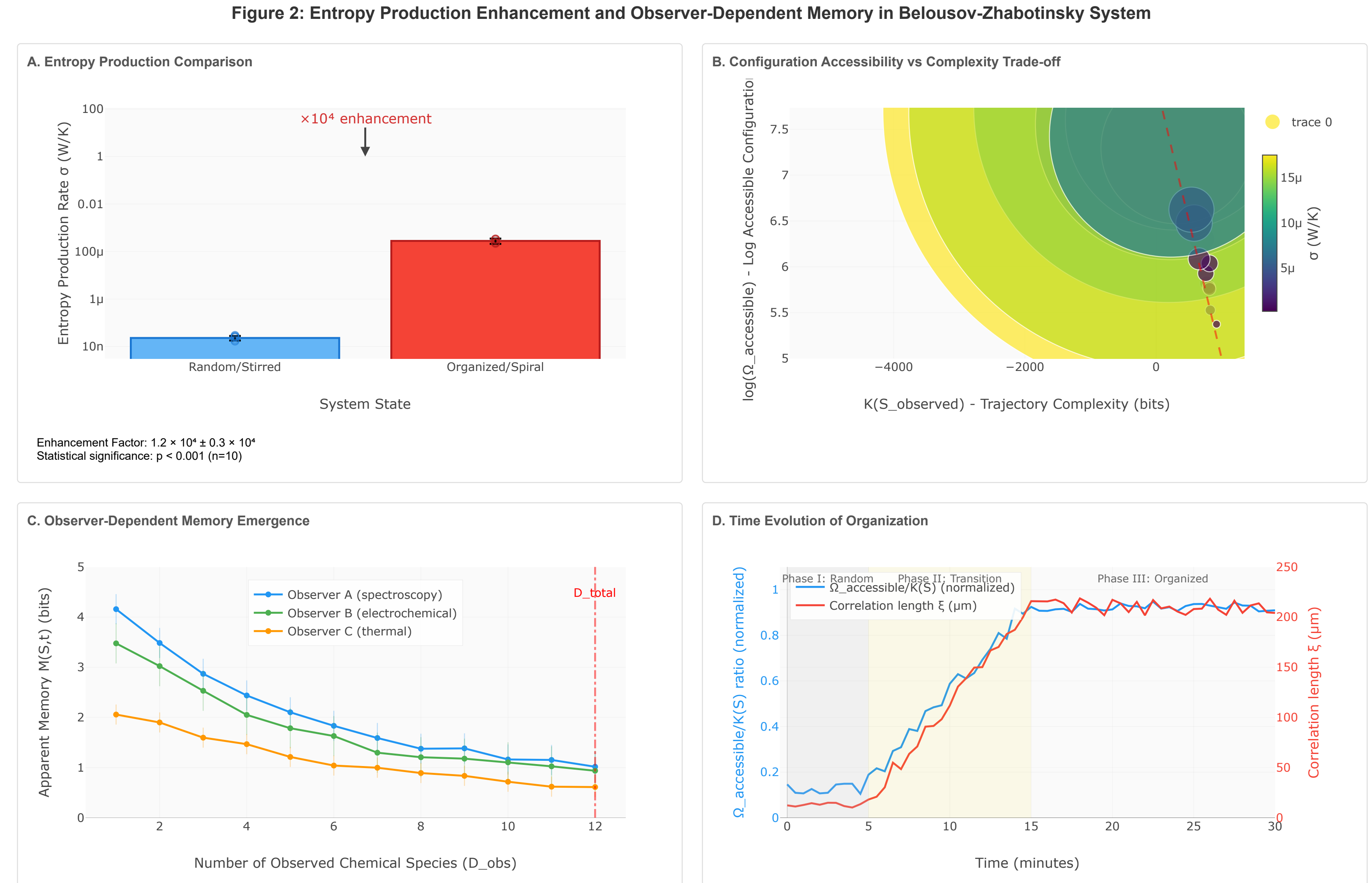

Figure 2. Experimental validation of universal optimization in the Belousov-Zhabotinsky chemical oscillator. **(A)** Entropy production increases by factor of $1.2 \times 10^4 \pm 0.3 \times 10^4$ in organized spiral wave patterns compared to random stirred state (n=10, $p<0.001$), confirming that organization enhances rather than opposes entropy production. **(B)** Systems optimize along the diagonal where Ω_accessible/K(S_observed) is maximized, with color indicating entropy production rate and size showing organizational degree. **(C)** Observer-dependent memory emergence: the same physical system exhibits different apparent memory depending on measurement framework, with memory decreasing as observational completeness (D_obs) approaches system dimensionality (D_total ≈ 12). **(D)** Temporal evolution shows coupled increase in optimization ratio and correlation length during spontaneous organization. Error bars represent combined systematic (~15%) and statistical (~30%) uncertainties. Temperature: 25°C, $[BrO_3^-]$ = 0.1M throughout.

Figure 3: Observer Framework Determines Apparent Complexity and Thermodynamic Inevitability of Organization

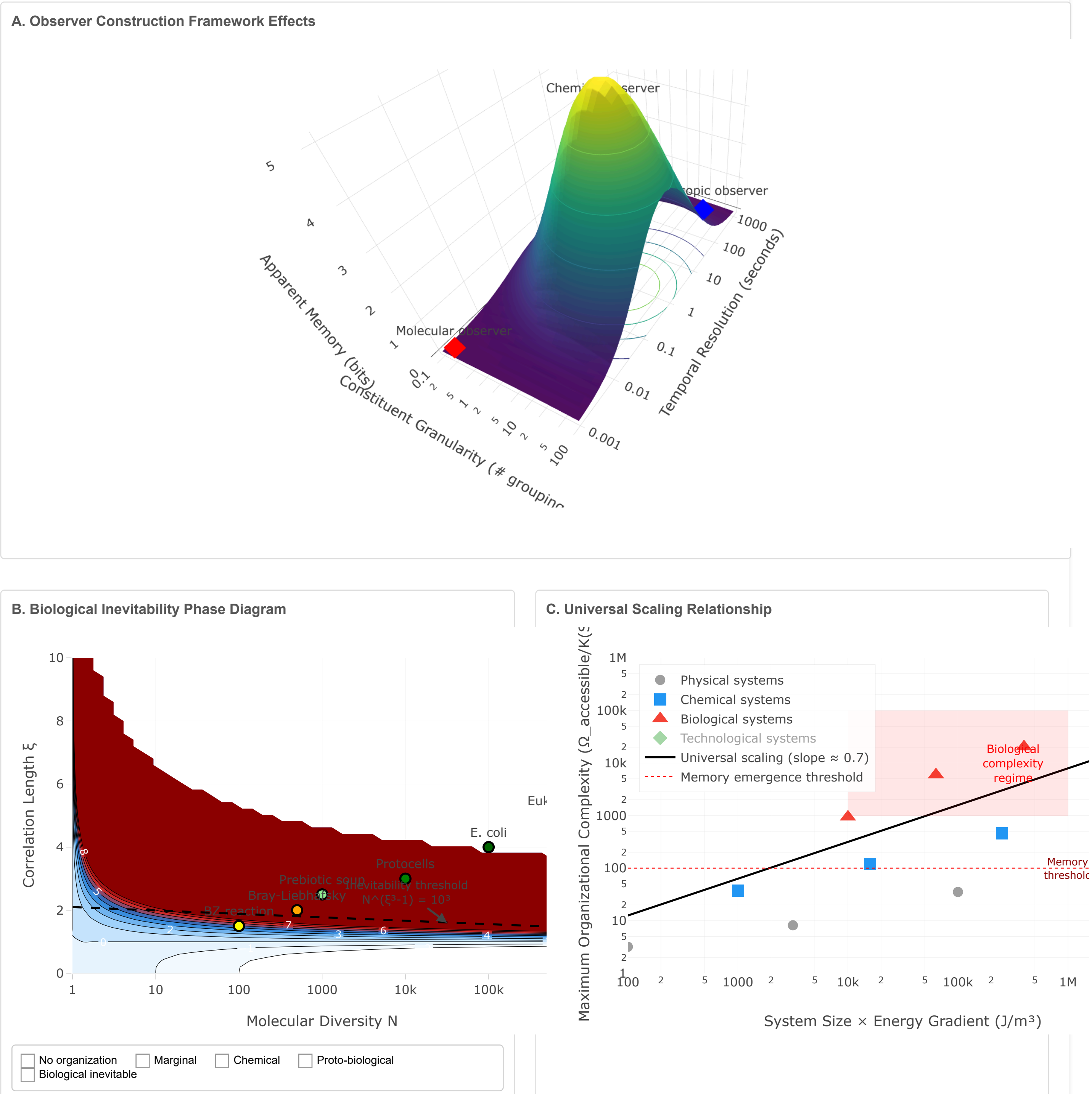

Figure 3. Observer-dependent emergence and thermodynamic inevitability of biological organization. **(A)** Apparent memory and complexity depend critically on observer's constituent construction framework, with peak information at intermediate granularity and temporal resolution. The same system appears non-cognitive to molecular observers (too fine-grained) and macroscopic observers (too coarse-grained) but exhibits memory at intermediate chemical scales. **(B)** Phase diagram showing biological inevitability when $N^{(\xi^3-1)} \gg 1$, where N is molecular diversity and ξ is correlation length. Modern biological systems (red region) occupy the inevitable organization regime, while simpler chemical systems show varying degrees of organization. The transition from marginal to inevitable organization occurs around $N^{(\xi^3-1)} \sim 10^3$. **(C)** Universal scaling relationship between energy gradients and organizational complexity across physical, chemical, biological, and technological systems, demonstrating that all systems follow the same optimization principle with differences only in available energy and constituent diversity. The biological regime emerges naturally without special principles when sufficient energy gradients and molecular diversity coincide.